**Summary of the USCB Advanced Test Reactor National Scientific Users Facility Irradiation Experiment –** G. R. Odette, T. Yamamoto, B. Sams, D. Klingensmith N. Cunningham (Department of Mechanical Engineering, University of California Santa Barbara) G. Waches, J. I. Cole, P. E. Murrey (Idaho National Laboratory)

## OBJECTIVES

The primary objective of this study is to create a large library of irradiated alloys, for a variety of specimen geometries, to address the scientific questions that include the following.

1. The effect of low dose (nominally 6 dpa peak) irradiations at 8 temperatures (nominally 288, 350, 400, 450, 500, 550, 650, and 750°C) on the basic microstructures and constitutive properties in disc multi-purpose coupons (DMC), cross comparing various alloys as well as examining model alloys.
2. The evolution of interface and bulk microstructure, microchemistry and micro-nanohardness in diffusion multiples (DM) specimens.
3. The effects on fracture toughness of radiation hardening at lower temperatures and microstructural and phase instabilities at higher temperatures for a subset materials and irradiation conditions.
4. The stability of the nanoscale Y-Ti-O features (NF) and nanostructured ferritic alloys (NFA) microstructures under high temperature irradiation.
5. Others mechanisms studies, including He transport and fate in-situ injection samples, including at high temperatures.

## SUMMARY

We have designed and prepared a comprehensive Advanced Test Reactor (ATR) irradiation experiment as part of a successful ATR National Scientific Users Facility (NSUF) proposal entitled *Characterization of the Microstructures and Mechanical Properties of Advanced Structural Alloys for Radiation Service: A Comprehensive Library of ATR Irradiated Alloys and Specimen.* A total of about 1400 specimens were fabricated and loaded at UCSB in 33 packets. Each packet has a unique outer profile and insulator design to minimize axial variations set by the Ar-He gas mixture and gap dimension. The packets were assembled at UCSB and subsequently loaded into 11 approximately 11 mm diameter capsule tubes at the Idaho National Laboratory (INL) in July, 2009. The experimental objective is to develop an integrated hardening/softening database from 288 to 750 ºC on 44 steels and model alloys irradiated up to 6 dpa. The experiment will also characterize the irradiation embrittlement of 6 alloys and support the development of small specimen fracture test methods including for interface fracture. The specimens will also support extensive microstructural and mechanism studies, including helium injection and diffusion multiple experiments. The irradiated specimens will form a “lending library” and sustain a number of future collaborations. The irradiation will be initiated in August of 2009 and completed in April of 2010.

## PROGRESS AND STATUS

### Scientific Objectives

The products of the ATR experiment will include the following items:

a. An unprecedented database on irradiation hardening (and softening) between 288 and 750°C from about 1.5 to 6 dpa for 6 TMS, 10 NFA and 1 austenitic alloys. The irradiation hardening will be primarily characterized by microhardness measurements, supplemented by tensile tests on a subset of materials. This will provide a database for refined fits of semi-empirical hardening models that we have developed. Since many alloys will be irradiated side-by-side, the database will also provide a unique opportunity to develop models for the effects of metallurgical variables on irradiation hardening. Combinations of special microhardness techniques that we have developed will be combined with the other deformation dominated fracture tests for a subset of alloys, such as tensile and shear punch measurements, and used to develop micromechanical models of constitutive, flow instability and failure ductility properties of the

irradiated alloys over a wide range of temperatures. Irradiations of TMS alloys at higher temperatures will provide a database for examining microstructural instabilities that can lead to softening (as well as non-hardening embrittlement - see below). Such instabilities are manifested as coarsening of precipitates and subgrains, recovery of dislocation and lath structures and precipitation of brittle phases, generally on the grain boundaries. There is growing evidence that irradiation and thermal instabilities interact synergistically. Thus the ATR mechanical property and microstructural data will be combined with thermal aging studies to provide the first systematic investigation of irradiation-thermal instability synergisms at higher temperatures.

b. Fracture mechanics studies using compact tension (CT) specimens in the framework of the Master Curve Method will be carried out on a subset of alloys to measure shifts in the 100 MPa√m reference temperatures, $\Delta T_o$. These tests will be supplemented by mini bend bar tests on other alloys. The irradiation will be used to further develop a new wedge loading chevron notch specimen, primarily intended to characterize the strength and toughness of interfaces. These small specimen methods can be used to evaluate test specific transition temperature shifts $\Delta T$ that can be adjusted to $\Delta T_o$ using calibrated micromechanical models.

c. Microstructural characterization on the irradiation-conditioned materials studies using a large suite of state of the art tools (SANS, TEM, APT, PAS and various X-ray based techniques). We will seek to establish a large international network of university and laboratory collaborators to assist in these studies. This could be enabled, for example, by providing small FIBed specimens that minimize limitations normally imposed by handling highly radioactive materials. In this sense, the ATR experiment will provide a "lending library" of specimens that can be examined by a large number of scientists using a variety of techniques. In addition to carrying out some of these studies ourselves, UCSB's role would be to encourage and help coordinate the collaborative research, to pool the information into a useful database and to combine it with mechanical property data to develop advanced microstructurally-based physical models of the deformation and fracture of irradiated alloys.

d. Model alloys and systems of various sorts are also included in the experiment. For example, a series of simple model alloys will be included to assess the effects of 0 to 18% Cr in simple Fe-Cr binary alloys over a wide range of irradiation temperatures. The experiment will probe the effect of Cr on both defect accumulation and $\alpha'$ precipitation including the effects of radiation enhanced diffusion (RED) and possible irradiation-induced non-equilibrium modifications of $\alpha$-$\alpha'$ phase boundaries. Other model materials include a set of pressure vessel steels, simple two to five constituent ferritic alloys, some maraging steels and model nanolayered metallic composites with engineered boundaries.

e. A very exciting and absolutely novel aspect of the ATR experiment will be the inclusion of so-called diffusion multiples (DM) that provide a "lab on a chip-combinatorial" type opportunity to characterize thermo-kinetic parameters of multiconstituent-multiphase alloys including mapping the phase diagrams and interdiffusion rates. DM are bonded assemblies of typically 3 elements, akin to more familiar and simpler binary diffusion couples. In the case of a diffusion couple made of primary elements, thermal aging provides information of equilibrium phase boundaries and interdiffusion rates along a binary tie line at a specified temperature. In the case of the diffusion multiple, this information is extended to ternary, quaternary and even higher order systems by creating corresponding multi-element inter-diffusion zones. These zones can be probed by a number of microstructural-microanalytical techniques as well as methods to probe physical and mechanical properties (e.g., using nanohardness). The large database produced by diffusion multiples will be analyzed to derive the thermodynamic and kinetic parameters used in computational materials codes like *Thermocalc* and *Dictra* and advanced models (e.g., phase field) of microstructural-microchemical evolutions. While the DM method is not new, it has never been applied to evaluation of alloy thermo-kinetics under irradiation, so the ATR irradiation present a unique new opportunity. Annealing diffusion multiple specimens will also help separate non-equilibrium effects of irradiation from radiation enhanced diffusion accelerated near equilibrium processes. Radiation enhanced diffusion will permit explorations of lower temperature thermodynamic regimes that are otherwise kinetically inaccessible due to slow thermal diffusion rates. Note that such databases are absolutely

essential for computational materials by design approaches to developing advanced high performance, radiation tolerant alloys.

f. In situ He generation experiments will also be carried out in the ATR irradiation. The thermal to fast neutron flux ratio is lower in ATR compared to HFIR and the peak dpa in the experiment is also lower. Thus the maximum He content in this case will be limited to about 150 appm. However this amount is sufficient to address issues of He transport and fate and will permit us to include newer and more advanced NFA than in the previous and ongoing HFIR irradiations over a wider range of temperatures. The ATR experiments will use thick Ni implantation foils to inject $\alpha$-particles into wedge shaped specimens from both sides to producing uniform He concentrations up to a thicknesses of ≈ 8 μm. The use of wedge specimens will also facilitate PIE since their end will be partially pre-thinned to near electron transparency.

### Test Matrix

The irradiation contains ≈ 1400 specimens of different types, composed of a wide variety of materials, which will provide a large body of microstructural and mechanical property data to address many key irradiation service questions. The irradiations will be carried out in the A10 position at ATR up to a maximum dose of ≈ 6 dpa. The specimens are loaded into 11 capsules, 10 out of which are irradiated at a time, to obtain the temperatures and doses specified in Table 1 for each of the experimental capsules. Baseline irradiation temperatures are 288, 550 and 750°C; smaller capsules will also be irradiated at 350, 400, 450 and 500°C.

Most specimens are simple DMC (0.2 mm thick and ≈ 10 mm in diameter) of more than 60 materials that are to be used for microstructural studies (TEM, SANS,…), measuring constitutive properties by advanced hardness techniques, shear punch tests (also making TEM discs), post irradiation annealing studies and disc bend (DB) fracture tests. The tentative alloy matrix consists of 6 tempered martensitic steels (TMS), 10 NFAs, 1 stainless steel (SS) and 28 model alloys (MA), 3 DM. Selected alloys are included in the form of sub-sized SS-J tensile specimens, disc tensile specimen (DTS), disc compact tension (DCT) fracture specimens, and deformation and fracture mini-beams (DFMB). The DM specimens, made of 3 joined elements (or different alloys), are used to study *radiation modified* inter-diffusion and phase formation processes, encompassing the entire phase diagram at the specified temperature. An advanced sub-sized dual chevron notched cantilevered beam specimen that is under development to provide higher constraint than standard fracture specimens of corresponding sizes, is included as well.

More detailed description and purposes of the materials and specimen types as well as irradiation conditions are give in the later sections.

### Materials of interest

In this study, six different classes of alloys and processing conditions are being investigated as summarized in Table 2 along with nominal compositions of the alloys. The study will focus on Fe-based alloys being considered for next generation reactor applications as both cladding and structural materials, and range from simple model alloys to complex commercially fabricated alloys. The following sections will highlight briefly the significance of each of these classes of samples.

Table 1 UCSB ATR Experiment Capsule Summary

| Capsule ID | Materials | Target Temp. | Nominal Target Dose |
|---|---|---|---|
| UCSB-1 | Mostly Fe-Based Metals | 288 ºC | 1.7 dpa |
| UCSB-2 | | 550 - 750 ºC | 2.3 to 4.2 dpa |
| UCSB-3 | | 350 - 550 ºC | 4.5 – 5.2 dpa |
| UCSB-4 | | 650 - 750 ºC | 5.6 – 5.9 dpa |
| UCSB-5 | | 350 - 500 ºC | 6.1 – 6.2 dpa |
| UCSB-6A* | | 288 ºC | 1.7 dpa |
| UCSB-6B* | | 288 ºC | 4.6 dpa |
| UCSB-7 | | 288 ºC | 6.0 – 6.1 dpa |
| UCSB-8 | | 288 ºC | 5.5 dpa |
| UCSB-9 | | 288 ºC | 4.0 – 5.0 dpa |
| UCSB-10 | | 350 – 500 ºC | 2.3 – 3.5 dpa |

* 6A runs for the first cycle only and is replaced with 6B that runs through the end of the project.

**Tempered Martensitic Steels (TMS):** These alloys, frequently referred to as ferritic-martensitic steels (F-M), include T91, HT9, NF616, F82H-IEA, F82H mod.3, and Eurofer 97. All but HT9 (≈12wt% Cr) have Cr content on the order of 8 to 9 wt%, and undergo a martensitic transformation following a austenitizing-normalizing tempering thermal treatments result a high strength and toughness. HT9 is the current primary cladding and duct candidate for liquid metal cooled burner reactors.. T91 and NF616 are two F-M alloys currently in use in fossil and other non-nuclear industries, and F82H and Eurofer 97 are alloys developed for fusion applications that have reduced long-term radioactivity permitting a more economical shallow surface burial waste disposal path. All of the alloys have BCC crystal structures generally manifest low swelling rate. Radiation induced shift of the ductile-to-brittle transition temperature (DBTT) is a major issue in using these F-M alloys in a irradiation environment and understanding embrittlement will be substantial focus of these studies.

**Nanostructured Ferritic Alloys (NFA):** The second set of materials are a series of primarily developmental alloys, all of which are Fe-based, that contain high densities of nanometer-scale dispersion strengthening features (NF). NFA have outstanding high temperature creep strength compared to conventional F-M alloys. There is considerable evidence that NFA are very radiation tolerant because NF act as sinks for radiation produced point defects and trap He in fins-scale harmless bubbles.

**Stainless Steels (SS)**: One cast austenitic stainless steel alloy was included in the experiment.

**Model Alloys (MA):** Simple model alloys were included for fundamental and developmental. These alloys range from pure iron to binary and ternary alloys, to complex model reactor pressure vessel steels. Information from these studies will help verification and validation of computer models being developed to predict irradiation effects in more complex systems.

**Diffusion Multiples (DM):** DM were included to permit the study thermo-kinetics in multi-element systems under irradiation over a range of temperature. They consisted of up to three diffusion bonded elements or alloys to promote subsequent interdiffusion and phase formation. The triple junction is a DM, while interfaces bonds represent diffusion couples (DC). Note Table 2a lists the primary DM combinations. However, W top and bottom caps were used in all cases, that also resulted in other DM and DC regions.

Table 2a Nominal Chemistry of Target Materials

| Material Category | Material ID | Cr | W | Mo | Ni | C | Ti | Y | V | Si | Fe | Other |
|---|---|---|---|---|---|---|---|---|---|---|---|---|
| Tempered Martensitic Steels (TMS) | T91 | 8.4 | - | 0.5 | - | 0.1 | - | - | - | - | bal. | |
| | HT-9 | 12.0 | 0.5 | 0.9 | 0.5 | 0.2 | - | - | 0.3 | 0.2 | bal. | |
| | NF616 | 8.8 | 1.9 | 0.5 | 0.2 | 0.1 | - | - | 0.2 | 0.2 | bal. | |
| | F82H IEA | 7.7 | 2.0 | - | - | 0.1 | - | - | 0.2 | 0.2 | bal. | |
| | F82H mod.3 | 7.7 | 2.0 | - | - | 0.1 | - | - | 0.2 | 0.2 | bal. | |
| | Eurofer 97 | 9.0 | 1.1 | - | - | 0.1 | - | - | 0.2 | 0.2 | bal. | |
| Nano-structured Ferritic Alloys (NFA) | MA956 | 20 | - | - | - | 0.04 | 0.4 | 0.5 | - | - | bal. | Al 4.5 |
| | MA957 | 14 | - | 0.3 | 0.1 | 0.1 | 1.0 | 0.25 | - | - | bal. | Al 0.1 |
| | PM2000 | 20 | - | - | - | 0.1 | 0.5 | 0.5 | - | - | bal. | Al 5.5 |
| | 14CrYWT-1150 | 14 | 3 | - | - | - | 0.4 | 0.25 | - | - | bal. | |
| | 14CrYWT-1000 | 14 | 3 | - | - | - | 0.4 | 0.25 | - | - | bal. | |
| | 9Cr-2WYT | 9.2 | 2.0 | - | - | 0.03 | 0.3 | 0.3 | - | 0.04 | bal. | |
| | 16Cr-2WYT | 16 | 1.8 | - | - | 0.03 | 0.3 | 0.3 | - | 0.04 | bal. | Al 4.6 |
| | 14CrYWT(H-milled) | 13 | 1.0 | - | - | - | 0.3 | 0.3 | - | - | bal. | |
| | 14CrYWT(Ar-milled) | 13 | 1.0 | - | - | - | 0.3 | 0.3 | - | - | bal. | |
| | 14CrYWT ORNL | 14 | 3 | - | - | - | 0.4 | 0.25 | - | - | bal. | |
| Stainless Steels (SS) | Cast SS | 17 | 13 | 2.5 | | | | | | | bal. | Mn 3; N 0.3 |
| Diffusion Multiple (DM) | Fe-Cr/W/Ti | 10 | 10 | - | - | - | 10 | 10 | - | - | bal. | |
| | Fe-Cr/W/Ni | 10 | 10 | 10 | - | - | - | - | - | - | bal. | |
| | Fe/Cu/Ni/W | 14 | - | - | 21 | - | - | - | - | 10 | bal. | |

Table 2b Nominal Chemistry of Target Materials (Model alloys)

| Material ID | Cr | W | Mo | Cu | Mn | Ni | C | P | Nb | V | Si | Fe | Other |
|---|---|---|---|---|---|---|---|---|---|---|---|---|---|
| JRQ | 0.12 | - | 0.50 | 0.14 | 1.4 | 0.82 | 0.1 | 0.01 | - | - | 0.2 | bal. | |
| LA | - | - | 0.55 | 0.40 | 1.3 | 0.00 | 0.1 | 0.00 | - | - | 0.2 | bal. | |
| LB | - | - | 0.55 | 0.40 | 1.3 | 0.18 | 0.1 | 0.00 | - | - | 0.2 | bal. | |
| LC | - | - | 0.55 | 0.41 | 1.4 | 0.86 | 0.1 | 0.00 | - | - | 0.2 | bal. | |
| LD | - | - | 0.55 | 0.38 | 1.3 | 1.25 | 0.1 | 0.00 | - | - | 0.2 | bal. | |
| LG | - | - | 0.55 | 0.00 | 1.3 | 0.74 | 0.1 | 0.00 | - | - | 0.2 | bal. | |
| LH | - | - | 0.55 | 0.11 | 1.3 | 0.74 | 0.1 | 0.00 | - | - | 0.2 | bal. | |
| LI | - | - | 0.55 | 0.20 | 1.3 | 0.74 | 0.1 | 0.00 | - | - | 0.2 | bal. | |
| OV1 | - | - | - | - | 1.6 | - | - | - | - | - | | bal. | |
| OV2 | - | - | - | - | 1.6 | 0.80 | - | - | - | - | | bal. | |
| OV3 | - | - | - | - | 1.6 | 1.60 | - | - | - | - | | bal. | |
| OV4 | 0.05 | - | - | - | 1.6 | 0.80 | - | - | - | - | | bal. | |
| OV5 | 0.05 | - | - | - | 1.6 | 1.60 | - | - | - | - | | bal. | |
| OV6 | 0.10 | - | - | - | 1.6 | 0.80 | - | - | - | - | | bal. | |
| OV7 | 0.10 | - | - | - | 1.6 | 1.60 | - | - | - | - | | bal. | |
| CM6 | - | - | 0.54 | 0.02 | 1.5 | 1.68 | 0.1 | 0.00 | - | 0.1 | | bal. | |
| F82H-1.4Ni | 7.7 | 2. | - | - | - | 1.4 | 0.1 | - | - | 0.2 | 0.2 | bal. | |
| Fe-3Cr | 3.0 | - | - | - | - | - | - | - | - | - | - | bal. | |
| Fe-6Cr | 6.0 | - | - | - | - | - | - | - | - | - | - | bal. | |
| Fe-9Cr | 9.0 | - | - | - | - | - | - | - | - | - | - | bal. | |
| Fe-12Cr | 12.0 | - | - | - | - | - | - | - | - | - | - | bal. | |
| Fe-15Cr | 15.0 | - | - | - | - | - | - | - | - | - | - | bal. | |
| Fe-18Cr | 18.0 | - | - | - | - | - | - | - | - | - | - | bal. | |
| SiC | - | - | - | - | - | - | 30 | - | - | - | 70 | - | |
| Maraging | 12 | | 1.4 | | 0.3 | 9.2 | | 0.03 | | | 0.3 | bal. | Al 1.6 |
| Ni/CuNb-1 | | | | 1.0 | | bal. | | | 1.0 | | | | |
| Ni/CuNb-2 | | | | 2.0 | | bal. | | | 2.0 | | | | |
| Ni/CuNb-3 | | | | 3.0 | | bal. | | | 3.0 | | | | |

**Specimen Types and Designs**

Nine unique geometries were included in the irradiation experiment, including:

- Disc multi-purpose coupons (DMC) that constitute the majority of the specimens. The DMC are nominally 8 mm (5/16 in) in diameter with both nominally 0.25 mm and 0.50 mm thickness dimensions. Smaller samples will be punched from the discs following irradiation.

- Diffusion Multiple (DM) 8 mm diameter discs with thickness dimensions from 2.25 to 2.75 mm as shown in Figure 1a.

- He implanter discs are DMC with a sharp ground and polished wedge over part of their circumference, producing a significant area thinner than 9 $\mu$m. The discs with wedges are placed between Ni foils as schematically illustrated in Figure 1b. He generated as $\alpha$-particles in Ni overlay foils under neutron irradiation are uniformly injected in the thin area.

- Subsize tensile specimens (SS-J2) shown in Figure 2a are 4 mm wide x 16 mm long and 0.5 mm thick. The gauge length is 5 mm. Special deformation tensile specimens with center-hole or dual offset gauge section notches shown in Figures 2b and 2c were also included.

- Disc compact tension (DCT) specimens shown in Figure 3, that will be used for fracture toughness testing, are 10 mm in diameter and 3.7 mm thick.

- Deformation and fracture mini-beam (DFMB) (not shown), that will also be used for studying fracture behaviour, are 1.67 mm square and 9.2 mm long and are pre-cracked to a crack length to width ratio of about 0.4.

- The chevron notch wedge (chevron) specimen, shown in Figure 4, are 5 mm high, 4 mm wide and 8 mm long. They will be used to investigate the effects of crack front lengths and constraint on fracture monolithic toughness in this experiment.

- Cylindrical compression (CC) specimens have a 2.0 mm diameter and 2.4 mm height.

The majority of the specimens are DMC.

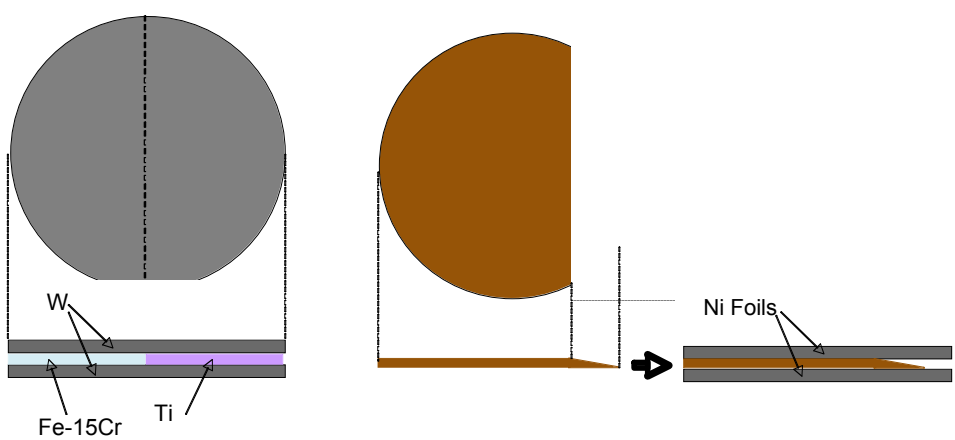


(a) (b)

Figure 1 Schematic drawings of: (a) diffusion multiple; and (b) He implanter discs.

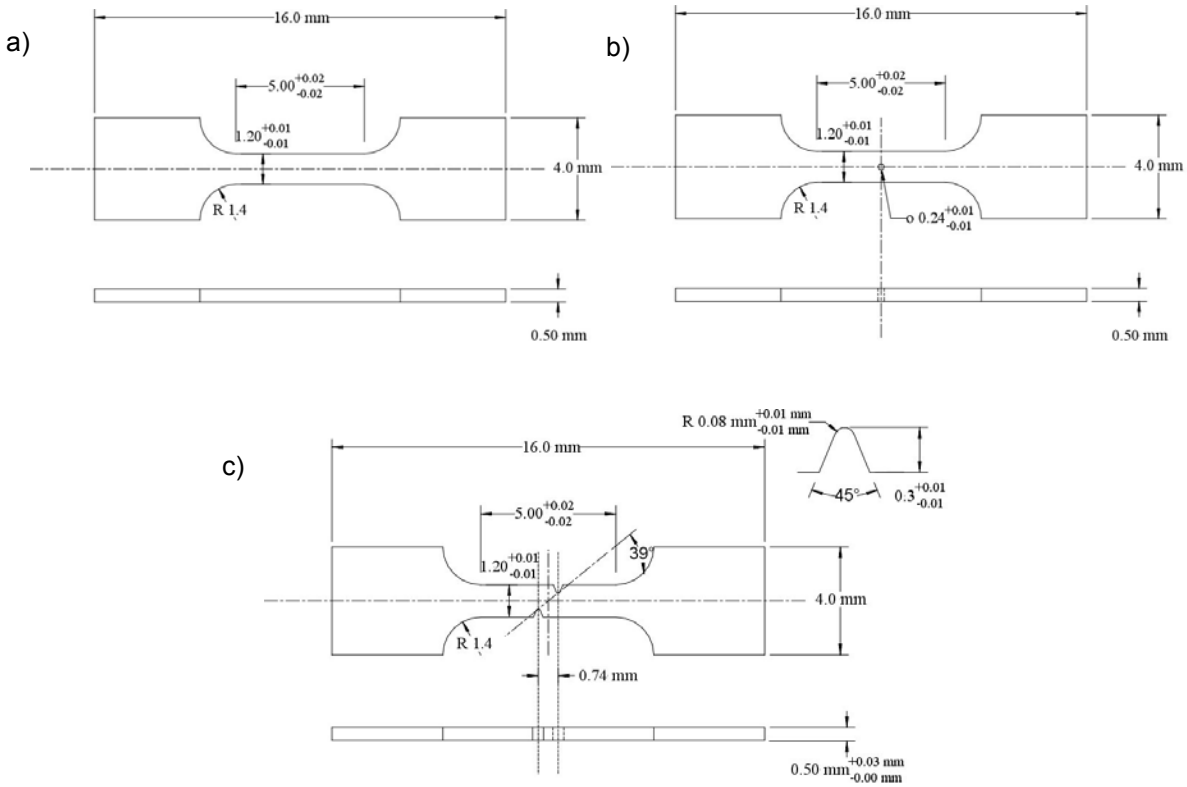


Figure 2 Drawings of three types of SSJ2 tensile coupon dog-bone specimens: a) plain, b) center-holed, and c) dual offset notched.

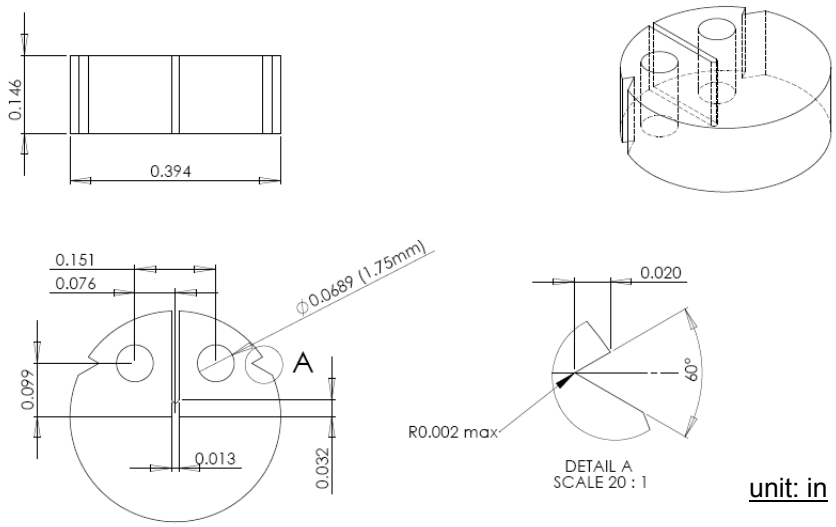


Figure 3 Drawing of the DCT specimen.

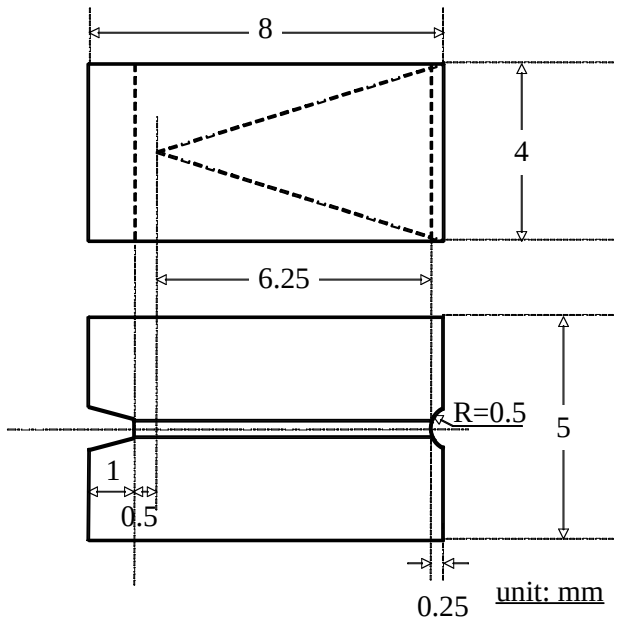


Figure 4 Schematics of a chevron notched wedge specimen.

**Irradiation Conditions**

Specimens were grouped into a total of 33 packets that were exposed at a target temperature over a narrow range of neutron fluence. Each packet was designed to minimize the axial temperature variations. An example of packet is shown in Figure 5a for the DMC specimens. The design features: 1) a “pill box” tube that contains a press-fit stack of DMC specimens; 2) a profiled outer shape to minimize temperature variations near the target temperature established by a precise gap and He-Ar gas mixture; 3) thick end plugs with thin stand-off pins that minimize axial heat flow. The packet and gap design was optimized by iterative finite element analysis (COMSL). Figure 5b illustrates the placement of a packet in a capsule; and Figure 5c shows an example of an optimized temperature distribution (± 6.5 ºC) for a 288ºC packet. Packets at each nominal temperature were placed in various positions inside the capsules and the capsule stack-ups so that they normally receive 3 (in 3 cases 2) peak peak fluences. Figure 6a shows the overall packet stack-up as a function of the power factor (PF). Figure 6b shows the corresponding flux versus fluence for the packets at each nominal irradiation temperature. The difference between the predicted and nominal temperatures for all the packets, ranging from 5 to 10 ºC, is shown in Figure 7. As shown in Table 1 and Figure 6b, capsule 6A is replaced by 6B after the first of four cycles. Capsule 6a receives 1.7 dpa at the near peak flux. Capsule 1, in the low flux region, receives the same dpa in 4 cycles, providing a basis to assess any dose rate effects over this flux range. Table 3 summarizes just types and the numbers of specimens for the irradiation conditions.

**Irradiation schedule and post-irradiation examination (PIE)**

The ATR irradiation will begin in August 2009 and will be completed in April 2010. The PIE will primarily be carried out in hot cell facilities of our national laboratory collaborator team. UCSB will lead the planning and execution of the PIE and subsequent analysis and evaluation of the resulting database. More detailed spreadsheet describing the materials, types and numbers of specimens and corresponding irradiation conditions, as well as a complete loading list, are available upon request.

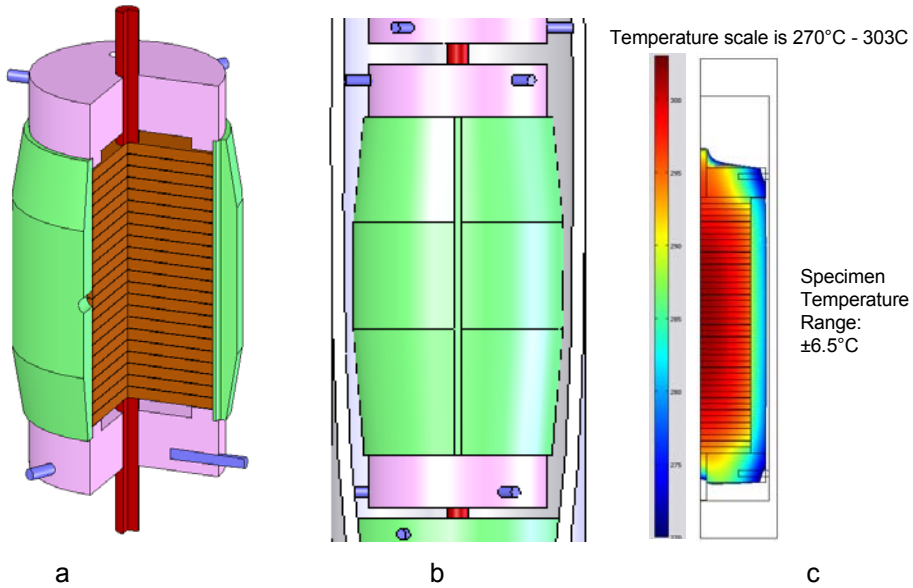


Figure 5 Illustration of (a) innovative “pill-box”-type packet to hold DMC (disc multipurpose coupon) specimens, (b) a special profiled “pill-box” shape to control gas gap heat conduction, and (c) the uniform thermal profile estimated for a 300 ºC capsule at high flux.

Table 3 Specimen types and numbers for the specified irradiation conditions

| Temperature (ºC) | Irr. Code | dpa | DMC-thin | DMC-thick | He-Imp | DM | B&C | SSJ | DTS | DCT | DFMB | CHW | Total |
|---|---|---|---|---|---|---|---|---|---|---|---|---|---|
| 288 | H | 5.6 | 36 | 113 | - | 3 | - | 36 | 9 | 25 | 48 | 6 | 276 |
| | M | 4.2 | - | 49 | - | - | - | 18 | - | - | - | - | 67 |
| | M@high-f | 4.6 | - | - | - | - | - | - | - | 8 | - | - | 8 |
| | L | 1.7 | 10 | 38 | - | - | - | - | - | - | - | - | 48 |
| | L@high-f | 4.6 | 8 | 53 | - | - | - | - | - | - | - | - | 61 |
| 350 | H | 6.1 | 22 | 52 | - | - | - | - | - | - | - | - | 74 |
| | M | 4.5 | - | 21 | - | - | - | - | - | - | - | - | 21 |
| | L | 3.5 | 10 | 36 | - | - | - | - | - | - | - | - | 46 |
| 400 | H | 6.2 | 18 | 52 | 14 | - | - | - | - | - | - | - | 84 |
| | L | 3.1 | 6 | 38 | - | - | - | - | - | - | - | - | 44 |
| | L | | | | | | | | | | | | 0 |
| 450 | H | 6.2 | 20 | 46 | - | - | - | - | - | - | - | - | 66 |
| | L | 2.7 | 10 | 26 | - | - | - | - | - | - | - | - | 36 |
| | L | | | | | | | | | | | | 0 |
| 500 | H | 6.2 | 9 | 52 | 14 | - | - | - | - | - | - | - | 75 |
| | L | 2.3 | 10 | 24 | - | - | - | - | - | - | - | - | 34 |
| | L | | | | | | | | | | | | 0 |
| 550 | H | 4.9 | 29 | 63 | 12 | 3 | - | 18 | - | - | 16 | - | 141 |
| | M | 4.0 | - | 27 | - | - | - | 18 | - | - | - | - | 45 |
| | L | 3.0 | 10 | 26 | - | - | - | - | - | - | - | - | 36 |
| 650 | H | 5.6 | 5 | 45 | 12 | 3 | - | 18 | - | - | - | - | 83 |
| | M | 3.3 | 4 | 15 | - | - | - | - | - | - | - | - | 19 |
| | L | 2.4 | 4 | 17 | - | - | - | - | - | - | - | - | 21 |
| 750 | H | 5.9 | 13 | 40 | 12 | 3 | - | - | - | - | - | - | 68 |
| | M | 3.6 | 2 | 16 | - | - | - | - | - | - | - | - | 18 |
| | L | 2.7 | 2 | 17 | - | - | - | - | - | - | - | - | 19 |
| Total | | | 228 | 866 | 64 | 12 | 0 | 108 | 9 | 33 | 64 | 6 | 1390 |

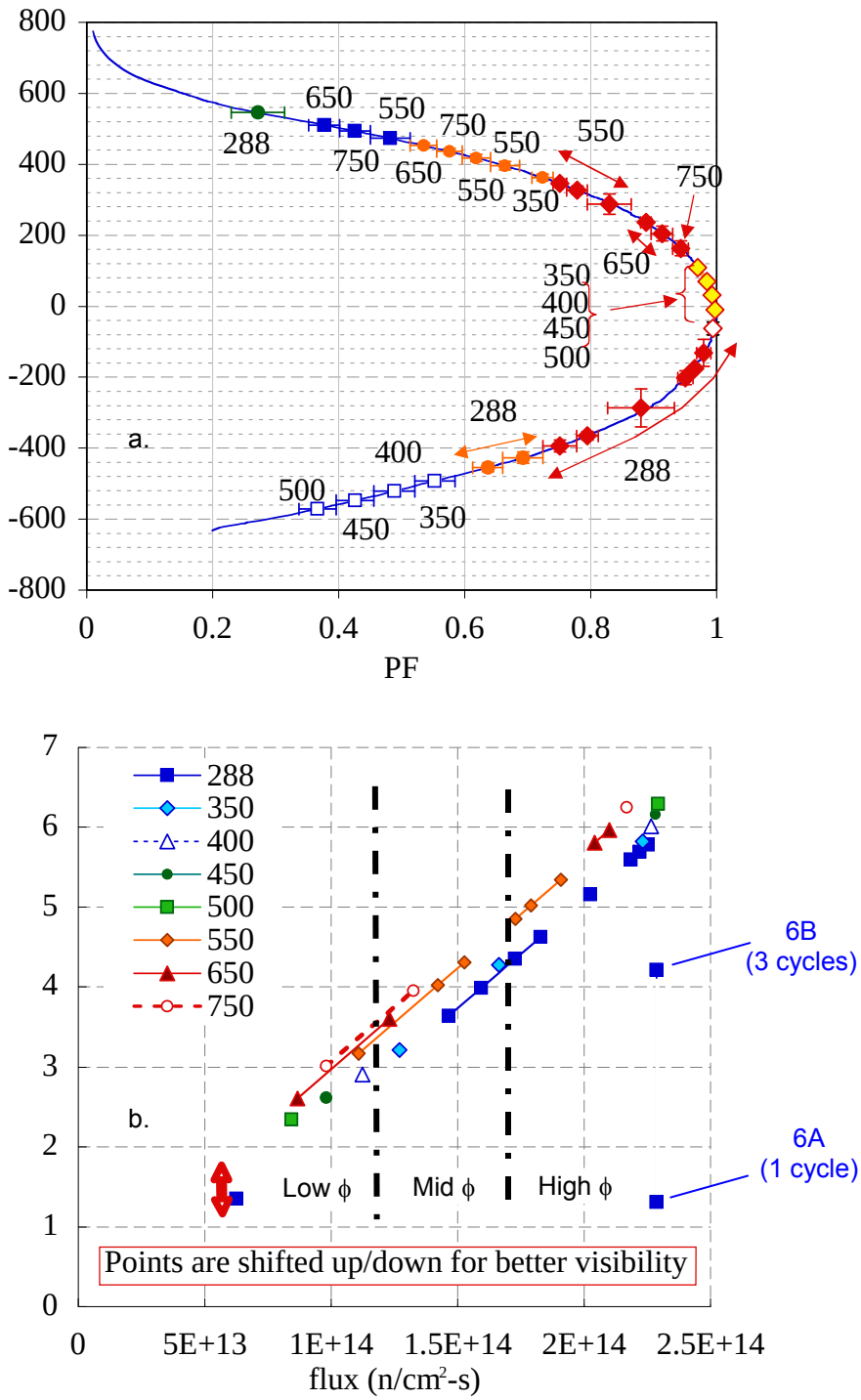


Figure 6 (a) Packet temperature assignment and power factors (PF) as a function of the packet location, (b) fluence – flux estimation of packets.

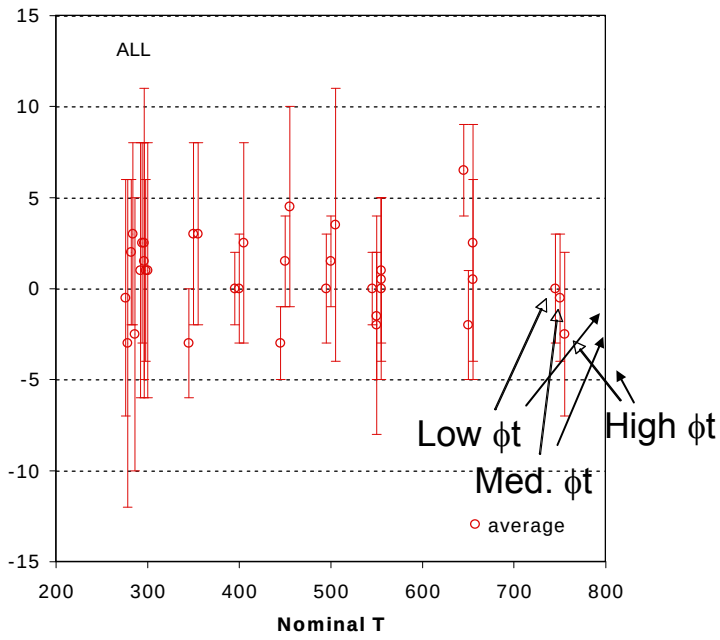


Nominal T (ºC)

Figure 7 Average and the range of difference between predicted and nominal temperatures for all the packets.

**Acknowledgement**

The authors are grateful to ATR NSUF program for all the technical support in designing and fabricating specimens and capsule parts. This research was also supported, in part, by the U. S. Department of Energy, Office of Fusion Energy Sciences, under contract DE-FG03-94ER54275, and by the U. S. Department of Energy, Office of Nuclear Energy, under contracts DE-FC07-05ID14663 and DE-FC07-07ID14825.